ISSN No: 2348-4845
International Journal & Magazine of Engineering, Technology, Management and Research
A Peer Reviewed Open Access International Journal

Design, Analysis, and Implementation of Solar Power Optimizer for DC Distribution System

Thatipamula Venkatesh
M.Tech, Power System Control and Automation,
Department of Electrical & Electronics Engineering,
Aurora's Technological and Research Institute,
Parvathapur ,Uppal, Hyderabad.

Mr.G.Vijay Krishna, M.Tech
Associate Professor & HOD,
Department of Electrical & Electronics Engineering,
Aurora's Technological and Research Institute,
Parvathapur ,Uppal, Hyderabad.

ABSTRACT:

This paper proposes a high step-up solar power optimizer (SPO) that efficiently harvests maximum energy from a photovoltaic (PV) panel then outputs energy to a dc-micro grid. Its structure integrates coupled inductor and switched capacitor technologies to realize high step-up voltage gain. The leakage inductance energy of the coupled inductor can be recycled to reduce voltage stress and power losses. A low voltage rating and low-conduction resistance switch improves system efficiency by employing the hill climb/ perturb & observe method for the maximum power point tracking (MPPT) algorithm. Because of its high tracking accuracy, the method is widely used in the energy harvesting of PV systems. laboratory prototypes of the proposed SPO that have an input voltage range of 20 to 40 V and a maximum PV output power of 340 V/300 W are applied. The highest PV power conversion efficiency is 95.7%. The maximum MPPT accuracy is 99.9%, and the full load average MPPT accuracy is 97.8%.

INTRODUCTION:

Fossil fuels continue to be depleted, and their use has been instrumental to climate change, a problem that grows more severe each year. A photovoltaic (PV) power generation system, which uses a renewable resource, has been extensively used in emergency facilities and in generating electricity for mass use. A conventional PV generation system is either a single- or a multi string PV array that is connected to one or several central PV inverters. Numerous series-connected PV modules are connected in the PV array to achieve the DC link voltage that is high enough to be connected to electricity through the DC AC inverter. However, the power reduction that is caused by the shadow effect is an inevitable problem in a centralized PV system. The use of a micro inverter or ac module has recently been proposed for individual PV panels. Although this discrete PV power generation solution may partially eliminate the shadow problem, a micro inverter structure constrains the system energy's harvesting efficiency and entails high costs. A solar power optimizer (SPO) was developed as an alternative to maximize energy harvest from each individual PV module.An SPO is used as a dc–dc converter with maximum power point tracking (MPPT), which increases PV panel voltage to optimum voltage levels for a dc micro grid connection or through a dc–ac inverter for electricity. This passes through an SPO to a dc micro grid system. A 400 V dc-micro grid system was proposed as an energy-efficient distribution option for data center systems and telecommunication facilities.The SPO attempts to improve the use of distributed renewable resources and lower system cost. It may also potentially improve the efficiency of PV systems, has an anti shadow effect, and can monitor the status of PV modules. Moreover, the dc-grid voltage is regulated by bidirectional inverter and battery tank. In case of low-loading condition, the redundant energy will store into battery or through bidirectional inverter to ac grid.A high step-up solar power optimizer (SPO) that efficiently harvests maximum energy from a photovoltaic (PV) panel then outputs energy to a dc-micro-grid. An SPO is used as a dc-dc converter with Maximum Power Point Tracking (MPPT), which increases PV panel voltage to optimum voltage levels for a dc micro-grid connection or through a dc-dc inverter for electricity Fig. below shows a single PV panel's energy. PV solar electricity together with solar thermal has the highest potential of all the renewable energies since solar energy is a practically unlimited resource, available everywhere.

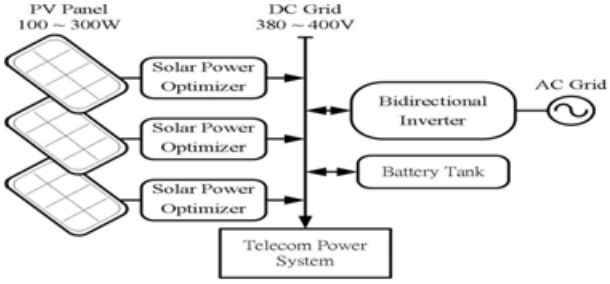

Fig: 1.1:Configuration of multiple parallel SPO for a dc-micro grid system.

ISSN No: 2348-4845
International Journal & Magazine of Engineering, Technology, Management and Research
A Peer Reviewed Open Access International Journal

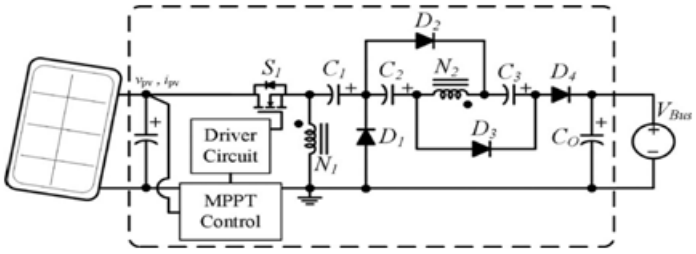

Fig.1.2: Configuration of the proposed SPO.

The proposed SPO is shown in Fig.1.2; its configuration is based on a high step-up dc–dc converter with an MPPT control circuit. The converter includes a floating active switch S and a coupled inductor T1 with primary winding N1, which is similar to the input inductor of a conventional boost converter capacitor C1, and diode D1 recycle leakage inductance energy from N1. Secondary winding N2 is connected to another pair of capacitors, C2 and C3, and to diodes D2 and D3. Rectifier diode D4 connects to output capacitor Co and load R. The duty ratio is modulated by the MPPT algorithm, which uses the hill climb/ perturb & observe method method that is employed in the proposed SPO. It detects PV module voltage Vpv and current Ipv to determine the increase and decrease in the duty cycle of the dc converter. Therefore, the MPP can be obtained by comparing instantaneous conductance I/V and incremental conductance dI/dV. The algorithm is programmed into TMS320LF2407A, a digital signal microprocessor.

1.1: THE PROPOSED CONVERTER FEATURES:

1) Its voltage conversion ratio is efficiently increased by using the switched capacitor and coupled inductor techniques.
2) The leakage inductance energy of the coupled inductor can be recycled to increase efficiency, and the voltage spike on the active switch is restrained.
3) The floating active switch isolates the PV panel's energy during non operating conditions, thereby preventing any potential electric hazard to humans or facilities. The MPPT control algorithm exhibits high-tracking efficiency; hence, it is widely used in the energy harvesting of PV systems.

1.2 : OPERATING PRINCIPLES:

The operating principles for continuous conduction mode (CCM) and discontinuous conduction mode (DCM) are presented in detail.

Fig illustrates a typical waveform of several major components in CCM operation during one switching period. To simplify the circuit analysis of the proposed converter, the following assumptions are made:
1) All components are ideal, except for the leakage inductance of coupled inductor T1, which is taken into account. On-state resistance RDS (ON) and all the parasitic capacitances of main switch S are disregarded, as are the forward voltage drops of diodes D1 to D4.
2) Capacitors C1 to C3 and Co are sufficiently large that the voltages across them are considered constant.
3) The equivalent series resistance (ESR) of capacitors C1 to C3 and Co , as well as the parasitic resistan ce of coupled inductor T1 , is neglected;
4) Turns ratio n of coupled inductor T1 windings is equal to N2 /N1 . The CCM operating modes are described as follows.

1.3. CCM OPERATION

1.3.1. MODE I [T0, T1]:

During this interval, switch S and diodes D2 and D3 are conducted; diodes D1 and D4 are turned OFF. The current flow path is shown in Fig.1.4(a). Magnetizing inductor Lm continues to release energy to capacitors C2 and C3 through secondary windingN2 of coupled inductor T1. Leakage inductance Lk 1 denotes the stored energy from source energy Vin. The energy that is stored in capacitor Co is constantly discharged to load R. This mode ends when increasing iLk1 is Equal to decreasing iLm at t = t1

$$vLm = Vin$$
$$\Delta iLm = VinLm(t1 - t0)$$

1.3.2. MODE II [T1, T2]:

During this interval, switch S and diode D4 are conducted. Source energy Vin is serially connected to C1, C2 , and C3 , and secondary winding N2 ; Lk2 discharges the energy that is stored in charge output capacitor Co and loads R. Meanwhile, magnetizing inductor Lm also receives energy from Vin . The current flow path is shown in Fig.1.4(b). This mode ends when switch S is turned OFF at t = t2.

$$\Delta iLm = (Vo - Vin - Vc1 - Vc2 - Vc3)\,(t2 - t1)/\,n \bullet Lm$$

ISSN No: 2348-4845
International Journal & Magazine of Engineering, Technology, Management and Research
A Peer Reviewed Open Access International Journal

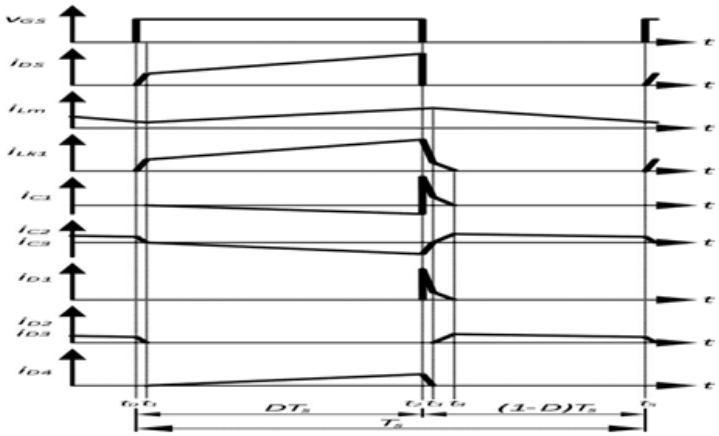

Fig.1.3: typical waveform of several major components in CCM operation during one switching period.

1.3.3. MODE III [T2, T3]:

During this transition interval, switch S and diodes D2 and D3 are turned OFF, and diodes D1 and D4 are conducted. The current flow path is shown in Fig.1.4(c). The energy stored in leakage inductance Lk 1 instantly flows through the diode D1 to charge capacitor C1 . The energy is released to magnetizing inductor Lm through coupled inductor T1 , which is serially connected to C1, C2 , and C3 , and secondary winding N2 ; Lk2 discharges the energy that is stored in charge output capacitor Co and loads R. This mode ends when decreasing iLk1 is equal to increasing iLm at t = t3

$$vLm = -Vc1$$
$$\Delta iLm = (-Vc1/I\,Lm)\,(t3 - t2)$$

1.3.4. MODE IV [T3, T4]:

During this interval, switch S and diode D4 are turned OFF, and diodes D1, D2, and D3 are conducted. The current flow path is shown in Fig.1.4(d). Leakage inductance Lk 1 continues to release energy to charge capacitor C1 through diode D1. Magnetizing inductor Lm through coupled inductor T1 transfers energy to capacitors C2 and C3 . The energy that is stored in capacitor CO is constantly discharged to load R. This mode ends when decreasing iLk1 is zero at t = t4

$$vLm = -Vc1$$
$$\Delta iLm = (-Vc1/I\,Lm)\,(t4 - t3)$$

1.3.5. MODE V [T4, T5]:

During this interval, diodes D2 and D3 are conducted. The current flow path is shown in Fig.1.4(e). Magnetizing inductor Lm constantly transfers energy to secondary winding N2 , and charges capacitors C2 and C3 . The energy that is stored in capacitor CO is constantly discharged to load R. This mode ends when switch S is turned ON at the beginning of the next switching period

$$vLm = (-V\,c2/\,n) = (-V\,c3/\,n)$$
$$\Delta iLm = (-V\,c2/\,n \bullet Lm)\,(t5 - t4) = (-V\,c3/\,n \bullet Lm)\,(t5 - t4)$$

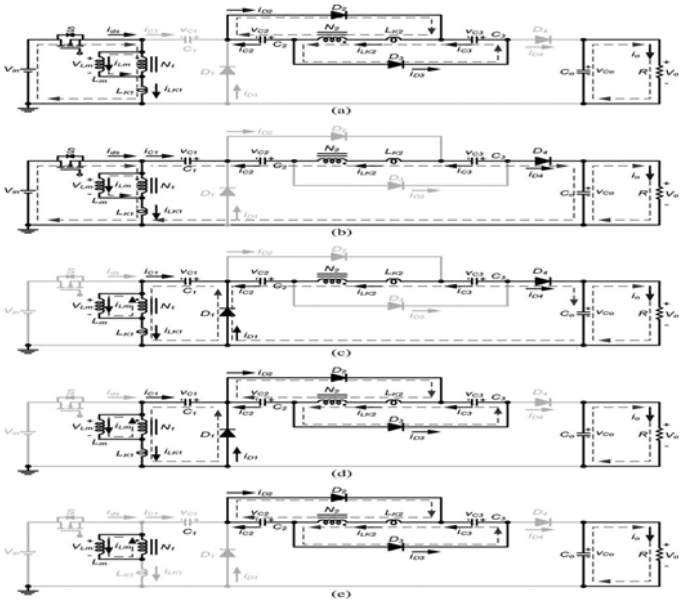

Fig.1.4.:Current flow path in five operating modes during one switching period in CCM operation: (a) Mode I, (b) Mode II, (c) Mode III, (d) Mode IV, and (e) Mode V.

1.4. DCM OPERATION

1.4.1. MODE I [T0, T1]:

During this interval, switch S and D4 are conducted, and diodes D1, D2, and D3 are turned OFF. The current flow path is shown in Fig.1.6(a). Magnetizing inductor Lm with leakage inductance Lk1 stores energy from source energy V in. Meanwhile, source energy Vin is also serially connected to capacitors C1, C2, and C3, and secondary winding N2 to charge capacitor Co and load R. This mode ends when switch S is turned OFF at t = t1

ISSN No: 2348-4845
International Journal & Magazine of Engineering, Technology, Management and Research
A Peer Reviewed Open Access International Journal

$$VLm = Vin = (VO-Vin-Vc1-Vc2-Vc3)/N$$
$$\Delta iLm = Vin\ Lm\bullet(t1-t0) = (VO-Vin-Vc1-Vc2-Vc3)/ n\bullet Lm\bullet(t1-t0)$$

1.4.2. MODE II [T1, T2]:

During this transition interval, switch S and diodes D2 and D3 are turned OFF, and diodes D1 and D4 are conducted. The current flow path is shown in Fig.1.6(b). The energy stored in leakage inductance Lk 1 instantly flows through the diode D1 to charge capacitor C1 ; this energy is also released to magnetizing inductor Lm through the coupled inductor T1 series that is connected to C1 , C2 , and C3 , secondary winding N2 , and Lk 2 to charge output capacitor Co and load R. This mode ends when decreasing iD 4 is zero at t = t2.

$$VLm = -Vc1$$
$$\Delta iLm = -Vc1 \bullet(t2-t1)\ n\bullet Lm$$

1.4.3. MODE III [T2, T3]:

During this transition interval, switch S and diode D4 are turned OFF, and diodes D1, D2, and D3 are conducted. The current flow path is shown in Fig.1.6(c). Leakage inductance Lk 1 continues to release energy to charge capacitor C1 through diode D1. Magnetizing inductor Lm transfers energy to capacitors C2 and C3 through coupled inductor T1. The energy stored in capacitor Co is constantly discharged to load R. This mode ends when decreasing iL k 1 is zero at t = t3

$$VLm = (-Vc1/n)=(-Vc2/n) = (-Vc2/n)$$
$$\Delta iLm = (-Vc1/ n\bullet Lm)\bullet(t3-t2) = (-Vc2/ n\bullet Lm)\bullet(t3-t2) = (-Vc3/ n\bullet Lm)\bullet(t3-t2).$$

1.4.4. MODE IV [T3, T4]:

During this interval, switch S, diodes D1 and D4 are turned OFF, and diodes D2 and D3 are conducted. The current flow path is shown in Fig. Magnetizing inductor Lm constantly transfers energy to secondary winding N2 and charges capacitors C2 and C3 . The energy that is stored in capacitor Co is constantly discharged to load R. This mode ends when decreasing iL m is zero at t = t4

$$vLm = (-Vc2/n) = (-Vc3/n)$$
$$\Delta iLm = (-Vc2/ n\bullet Lm) \bullet (t5-t4) = (-Vc2/n) \bullet(t4-t3)$$

1.4.4. MODE IV [T3, T4]:

During this interval, switch S, diodes D1 and D4 are turned OFF, and diodes D2 and D3 are conducted. The current flow path is shown in Fig. Magnetizing inductor Lm constantly transfers energy to secondary winding N2 and charges capacitors C2 and C3 . The energy that is stored in capacitor Co is constantly discharged to load R. This mode ends when decreasing iL m is zero at t = t4

$$vLm = (-Vc2/n) = (-Vc3/n)$$
$$\Delta iLm = (-Vc2/ n\bullet Lm) \bullet (t5-t4) = (-Vc2/n) \bullet(t4-t3)$$

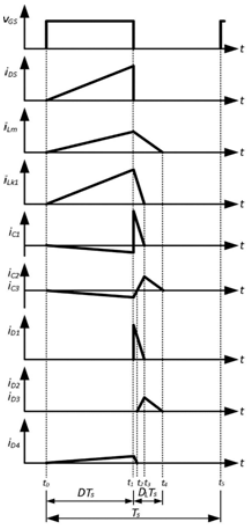

Fig: 1.5

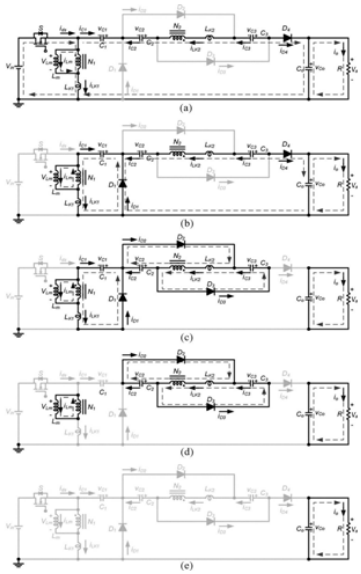

Fig: 1.6

Fig: 1.5.Typical waveforms of the proposed converter during DCM operation. Fig: 1.6. Current flow path in five operating modes during one switching period in DCM operation: (a) Mode I, (b) Mode II, (c) Mode III, (d) Mode IV, and (e) Mode V.

ISSN No: 2348-4845
International Journal & Magazine of Engineering, Technology, Management and Research
A Peer Reviewed Open Access International Journal

MAT LAB RESULTS

1.7 INPUT VOLTAGE

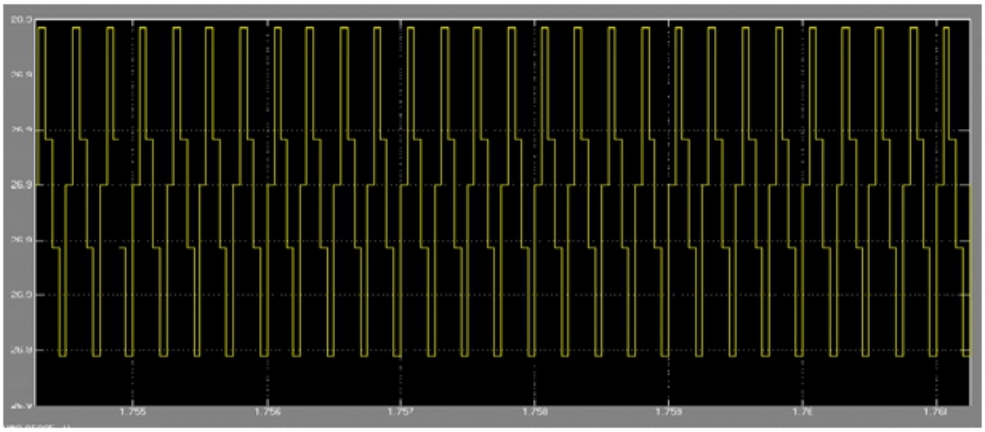

1.8 OUTPUT VOLTAGE

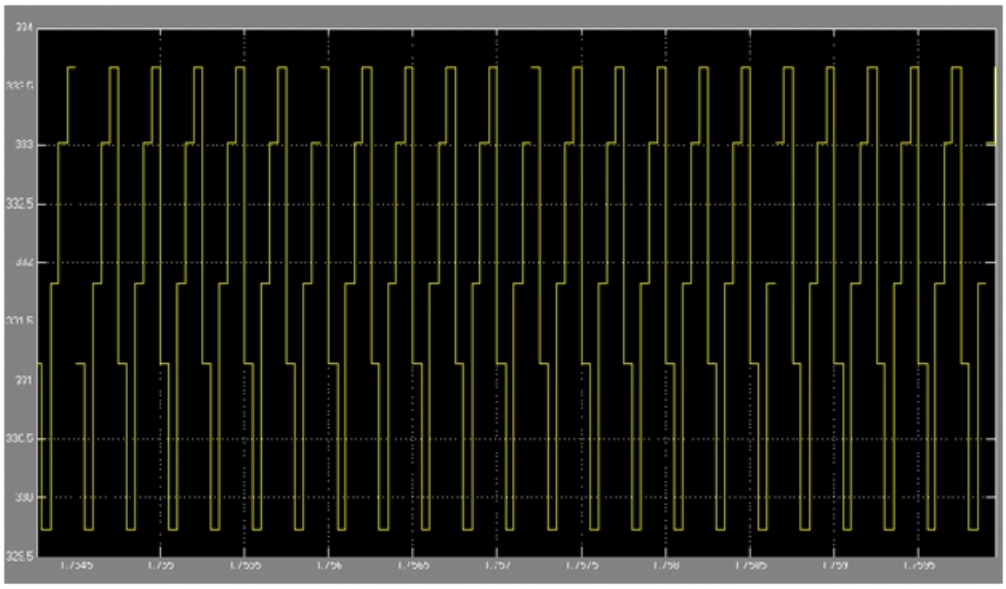

CONCLUSION:

The high step-up SPO uses the coupled inductor with an appropriate turn's ratio design and switched-capacitor technology to achieve a high-voltage gain that is 12.5 times higher than the input voltage. Because the leakage inductance energy of a coupled inductor is recycled and the voltage stress across the active switch S is constrained, the low RDS (ON) of active switch can be selected to improve maximum efficiency up to 96.7%. As a result, full load efficiency reaches 92.8%. The highest MPPT accuracy is 99.9% and the highest average accuracy is 97.9% at P PV = 150 W. A 300 W SPO with a high step-up voltage gain and MPPT functions are implemented and verified

REFERENCES:

[1] Y. Fang and X. Ma, "A novel PV micro inverter with coupled inductors and double-boost topology," IEEE Trans. Power Electron., vol. 25, no. 12,pp. 3139–3147, Dec. 2010.

[2] A. Ch. Kyritsis, E. C. Tatakis, and N. P. Papanikolaou, "Optimum design of the current-source flyback inverter for decentralized grid-connected photovoltaic systems," IEEE Trans. Energy Convers. , vol. 23, no. 1, pp. 281–293, Mar. 2008.

ISSN No: 2348-4845
International Journal & Magazine of Engineering, Technology, Management and Research
A Peer Reviewed Open Access International Journal

[3] P. Tsao, "Simulation of PV systems with power optimizers and distributed power electronics," in Proc. IEEE Photovolt. Spec. Conf., Jun. 2010, pp. 389–393.

[4] D. D.-C. Lu and V. G. Agelidis, "Photovoltaic-battery-powered DC bus system for common portable electronic devices," IEEE Trans. Power Electron , vol. 24, no. 3, pp. 849–855, Feb. 2009

[5] L. Zhang, K. Sun, Y. Xing, L. Feng, and H. Ge, "A modular grid-connected photovoltaic generation system based on DC bus," IEEE Trans. Power Electron, vol. 26, no. 2, pp. 523–531, Feb. 2011.

[6] S.M.Chen,K.R.Hu,T.J.Liang,L.S.Yang,andY.H.Hsieh ,"Implementation of high step-up solar power optimizer for DC micro grid application," inProc. IEEE Appl. Power Electron Conf., Feb. 2012, pp. 28–32.

[7] A.Pratt, P. Kumar, and T. V. Aldridge, "Evaluation of 400 V DC distribution in telco and data centers to improve energy efficiency," in Proc. IEEE Int. Telecommun. Energy Conf. , Sep./Oct. 2007, pp. 32–39.

[8] L. Zhang, K. Sun, Y. Xing, L. Feng, and H. Ge, "A modular grid-connected photovoltaic generation system based on DC bus," IEEE Trans. Power Electron., vol. 26, no. 2, pp. 523–531, Feb. 2011.